A Unified Machine Learning Method for Task-related and Resting State fMRI data Analysis

Xiaomu Song[1] and Nan-kuei Chen[2]

***Abstract*— Functional magnetic resonance imaging (fMRI) aims to localize task-related brain activation or resting-state functional connectivity. Most existing fMRI data analysis techniques rely on fixed thresholds to identify active voxels under a task condition or functionally connected voxels in the resting state. Due to fMRI non-stationarity, a fixed threshold cannot adapt to intra- and inter-subject variation and provide a reliable mapping of brain function. In this work, a machine learning method is proposed for a unified analysis of both task-related and resting state fMRI data. Specifically, the mapping of brain function in a task condition or resting state is formulated as an outlier detection process. Support vector machines are used to provide an initial mapping and refine mapping results. The method does not require a fixed threshold for the final decision, and can adapt to fMRI non-stationarity. The proposed method was evaluated using experimental data acquired from multiple human subjects. The results indicate that the proposed method can provide reliable mapping of brain function, and is applicable to various quantitative fMRI studies.**

I. INTRODUCTION

Blood oxygenation level dependent (BOLD) contrast functional magnetic resonance imaging (fMRI) plays an important role in advancing the understanding of brain function under a task condition or resting state. Reliable mapping of brain function in the task or resting state remains a challenge because BOLD signals typically exhibit a low signal-to-noise ratio, especially in the resting state.

Most existing fMRI-based brain mapping tools rely on statistical approaches such as hypothesis test, which implicitly assumes a probability distribution for features/statistics extracted from fMRI data, and identifies "active" or functionally "connected" brain regions using a predefined significance threshold. A voxel is identified as "active" or "connected" if its task-related signal fluctuation or resting state statistical measure exceeds the threshold. The selection of probability distributions and thresholds are usually based on experience or ad hoc, and no single model or thresholding approach has been approved to be optimum [1]. Due to fMRI non-stationarity, fMRI data may exhibit significant intra- and inter-subject variation even under a same experimental condition. Consequently, a fixed threshold cannot adapt to the variation of signal and noise characteristics, and is not reliable to provide a differentiation between active/connected and inactive/unconnected voxels [2].

[1]X. Song is with the Department of Electrical Engineering, Widener University, Chester, PA 19013 USA xmsong at widener.edu

[2]N.-K. Chen is with the Brain Imaging and Analysis Center, Duke University Medical Center, Durham, NC 27710, USA nankuei.chen at duke.edu

In our previous study [3], a data driven support vector machine (SVM)-based method was developed for reliable mapping of brain activation for individual subjects under different stimuli tasks. The method can explore a true boundary between active and inactive voxels in a feature space, and adapt to the intra- and inter-subject variation without using a fixed threshold for the final decision. Based on the previous work, we proposed a SVM-based method that unifies the analysis of task-related and resting state fMRI data into one framework. The method can be used for various quantitative fMRI studies.

II. PROPOSED METHOD

A. Problem Formulation

A recent study of brain activation location involving 31724 subjects from 8637 experiments (recorded in the BrainMap database [4]) shows that functionally connected voxels in a specific network constitute less than 50% of all brain voxels [5]. Considering a close correspondence between resting state networks and active functional networks under different task conditions revealed in a recent study [6], this observation applies to both task-related and resting state studies, and forms the basic assumption of the proposed method. With this assumption, the mapping of active voxels in a task condition, or a functional connectivity network in the resting state, can be considered as an outlier detection process, where "outliers" correspond to active or connected voxels.

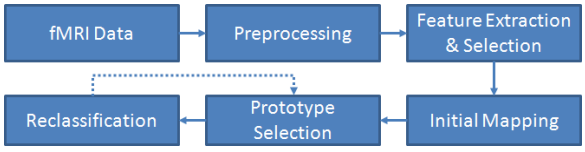

Fig. 1. The block diagram of the proposed method.

Fig. 1 shows the block diagram of the proposed method. The input fMRI data are first preprocessed to remove subject movement artifacts and low frequency drift, and filtered spatially and temporally. Multiple features are extracted from each voxel. An offline feature selection is performed to select most representative features to represent each voxel. Based on the selected features, One-class SVM (OCSVM) is used to provide an initial mapping. The prototype selection aims to identify voxels that are correctly classified by OCSVM. The identified voxels are used to train a two-class SVM (TCSVM) to reclassify all voxels to obtain a refined activation/connectivity map. The prototype selection and TCSVM

978-1-4244-7929-0/14/$26.00 ©2014 IEEE

reclassification can be repeated multiple times till there is no more change in the final mapping results.

B. Preprocessing

Small subject movement artifacts in fMRI data are first attenuated using a 2D rigid body registration method [7]. Then the data are spatially smoothed using a wavelet domain Bayesian noise removal method [8]. For task-related data, the expected haemodynamic response (HR) is estimated by convolving the experimental paradigm with the canonical haemodynamic response function used in SPM [9]. For resting state data, a low-pass filtering at a cut-off frequency of 0.1 Hz is performed to extract low frequency fluctuations of interest in the resting state, and a seed is selected from a brain region that is part of a network of interest.

C. Feature Extraction and Selection

Based on the expected HR or seed, multiple candidate features are extracted from each voxel's time course (TC). For task-related data, the candidate features include: the maximum intensity of the TC, p-value of the t-test, the average, maximum and minimum correlation coefficients (cc) between the voxel and other voxels within its 2^{nd}-order neighborhood, the average signed extreme value and delay of the cross correlation functions (ccf) between them, the cc between the TC and expected HR, the signed extreme value and its delay of the ccf between the TC and HR. For resting state data, the candidate features consist of: the cc between the seed and voxel, the maximum intensity of the voxel's TC, the signed extreme value and delay of the ccf between the seed and voxel, p-value of the t-test, the average, maximum and minimum cc between the seed and voxels within the 2^{nd}-order neighborhood, the average signed extreme value and delay of the ccf between the seed and voxels in the neighborhood, and the average, maximum and minimum cc between the voxel and other voxels within its neighborhood. All features are normalized between 0 and 1. Other features that could facilitate the SVM learning can also be added to the analysis.

Not all features contribute to the analysis. An offline feature selection is performed to identify most representative features [10]. It measures the contribution of each candidate feature by quantifying its effect on the construction of the SVM classification hyperplane in a feature space. Given the d^{th} candidate feature, its contribution I_d is estimated by an integration of the first derivative of the SVM decision function f_c with respect to the feature x_i^d around the hyperplane, and is approximated by [10]:

$$I^d \approx \sum_{i=1}^{N_{SV}} |\frac{\partial f_c}{\partial x_i^d}| = \sum_{i=1}^{N_{SV}} |\sum_{j=1}^{N_{SV}} \alpha_j y_j K^d(\mathbf{x}_j, \mathbf{x}_i)|, \quad (1)$$

where N_{SV} is the number of support vectors, $\mathbf{x}_i$ is the i^{th} support vector, x_i^d is the d^{th} feature of $\mathbf{x}_i$, $y_j \in \{-1, +1\}$ is the class label of $\mathbf{x}_j$, and α_j is the Lagrange multiplier defined in the SVM formulation [11]. $K(\mathbf{x}_j, \mathbf{x}_i)$ is a kernel defining a dot product between projections of $\mathbf{x}_i$ and $\mathbf{x}_j$ in a feature space [12], and $K^d(\mathbf{x}_j, \mathbf{x}_i)$ is the first derivative of the kernel regarding the d^{th} dimension evaluated at $\mathbf{x}_i$. A larger I^d value indicates a greater contribution to the SVM learning, and the top r features with the largest I^d value are used to form a feature vector to represent each voxel as the input to the following step.

D. Initial Mapping

The initial mapping of active/connected voxels is implemented as the outlier detection process via OCSVM. OCSVM learns a linear classification hyperplane in a feature space to separate a pre-specified fraction of data with the maximum distance to the origin [13]. The OCSVM parameter ν determines an upper bound of outliers, and is task-, network-, and subject-dependent. It cannot be accurately set due to the intra- and inter-subject variation. It is expected that the proposed method is not sensitive to inaccurate settings of ν. Based on our previous study [3], the following strategy is used to set ν: (1) If ν is unknown, ν is set to be relatively large but less than 0.5 to obtain a sufficient detection sensitivity. (2) If ν is approximately known *a priori* from previous studies, a range of ν is defined and any value within this range can be used.

Kernel methods can be used to implement nonlinear OCSVM [12]. In this work, the radial basis function (RBF) kernel is used that is defined as: $K(\mathbf{x}_i, \mathbf{x}_j) = e^{-\gamma\|\mathbf{x}-\mathbf{x}_i\|^2}$, where γ is the kernel width parameter. A large γ value corresponds to a small kernel width that introduces more nonlinearity to the analysis than a large kernel width. The kernel width may significantly affect the classification performance. In practice, γ is either experientially determined or estimated by cross validation.

E. Prototype Selection

A prototype consists of a feature vector representing a voxel and its class label (active/connected vs. inactive/unconnected). Due to inaccurate settings of ν, OCSVM results may contain a significant number of mis-detections. Prototype selection aims to identify correctly classified voxels for the TCSVM training. Since active/connected voxels are spatially grouped together at multiple anatomic sites, we may use graph-based spatial domain editing methods to remove spatially isolated mis-detections [14]. However, if mis-detections are also spatially grouped together, spatial domain operations are not sufficient to remove mis-detections. In such cases, the feature space distribution of the prototypes should be considered. In this work, a combined spatial and feature domain prototype selection is proposed.

The Gabriel graph can be used to describe a voxel's spatial relationship to its neighbourhood [14]. Given n points $Z = \{z_1, z_2, \cdots, z_n\}$ in a q-dimensional feature space R^q, a Gabriel graph $G(V, E)$ is a proximity graph with a set of vertices $V = Z$ and edges E, such that $(z_i, z_j) \in E$ if and only if the triangle inequality: $d(z_i, z_j) \leq \sqrt{d^2(z_i, z_k) + d^2(z_j, z_k)}$ is satisfied, where $z_k \in Z$, and d is the Euclidean distance in R^q. When Z is the spatial coordinates of a voxel, q is equal to 2. Given the 2^{nd}-order neighborhood of z_i, if its label is not dominant in

the neighborhood, the i^{th} voxel will be excluded from the training data based upon the Gabriel graph's 1^{st}-order graph editing technique with voting strategy [14].

After this operation, all voxels remaining in the training data are examined in the feature space. If s_i is the feature space distance between the i^{th} voxel and the OCSVM classification hyperplane, when $s_i < 0$, the voxel is classified as active/connected, and when $s_i > 0$, it is identified as inactive/unconnected. If $s_o < 0$ denotes the maximum distance of active/connected voxels to the hyperplane, and $s_m > 0$ is the maximum distance of inactive/unconnected voxles to the hyperplane, the following feature space prototype selection procedure is proposed: If the voxel is classified as active/connected and

$$s_i \leq (1.0 - e^{-\eta\nu})s_o, \tag{2}$$

or it is classified as inactive/unconnected and

$$s_i \geq (1.0 - e^{-\lambda\nu})s_m, \tag{3}$$

where η and λ control the fraction of voxels that are close to the hyperplane and should be removed, then this voxel is highly possible to be correctly classified and selected for the TCSVM training. The values of η and λ can be experimentally determined.

F. TCSVM Training and Classification

The selected prototypes are used to train a TCSVM to reclassify all voxels and obtain a refined activation/network map. TCSVM is a supervised learning tool that aims to estimate a linear classification hyperplane in a feature space so that two classes can be maximally separated [11]. The TCSVM training allows training errors with a parameter C controlling a tradeoff between the hyperplane complexity and training errors. The RBF kernel can be used to implement nonlinear TCSVM. The TCSVM output can be transferred to probability measures [15]. If p_i^o and p_i^m indicate the probability of the i^{th} voxel to be active/connected and inactive/unconnected, then if $p_i^o > p_i^m$, the voxel is classified as active/connected, and if $p_i^m > p_i^o$, then it is classified as inactive/unconnected. To favor a high generalization performance, the TCSVM parameters are carefully set with a large RBF kernel width and small C values.

III. Experiments

The proposed method was evaluated using experimental fMRI data acquired from task-related and resting state experiments. A task-related experiment was performed on a healthy adult using a 3 Tesla GE system at Duke University Medical Center. Four data sets were acquired from the subject on the same day using T_2^*-weighted parallel echo planar imaging (EPI) with an acceleration factor of 2, while the subject was performing a right finger-tapping motor task with a blocked-design paradigm, which consisted of four 25 s task blocks and five 25 s off blocks. EPI parameters included a repetition time (TR) of 2 s, an echo time (TE) of 30 ms, and a flip angle of 90°. 30 axial-slices were collected for each volume with 4 mm slice thickness and 1 mm gap, field of view (FOV) was 24 cm×24 cm, and image matrix was 120×120. The resting state experiments were implemented using the same scanner and head coil. Two data sets were collected from two subjects using a T_2^*-weighted EPI sequence with SENSE acceleration factor of 2 while the subjects were instructed to look at a crosshair. The scan time for each run was 4 min, with a TR of 2 s and a TE of 25 ms. 35 axial-slices were collected for each volume with 3 mm slice thickness. FOV was 24 cm× 24 cm, and image matrix was 64×64. The experiments were compliant with the standards established by the Institutional Review Boards of Duke University.

IV. Results

A. Task-related Experiments

Fig. 2 shows the activation maps overlaid on an individual slice generated for the motor task stimulation using the proposed method with ν=0.25, 0.28, and 0.35, respectively. There are 2127 voxels in this slice involved to the analysis. The increase of ν is 10%, but only 5 more voxels (0.2% increase) were identified to be active, indicating approximately 50 times less dependence on ν than OCSVM.

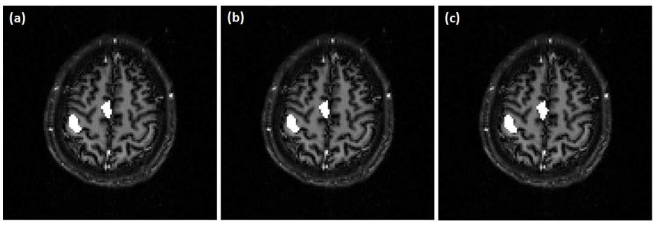

Fig. 2. Activation maps generated for the motor task paradigm by the proposed method with (a) ν=0.25, (b) ν=0.28, and (c) ν=0.35.

B. Resting State Experiments

Fig. 3 shows part of default mode network (DMN) identified from one data set acquired from the resting state experiment. A 2×2 voxels seed was manually identified in the ventral anterior cingulate cortex (VACC) region. Fig. 3 (a)-(d) are the DMN maps detected using the proposed method with ν=0.31, 0.37, 0.39, and 0.41, respectively. 2031 voxels were used in the processing, and only 10 more voxels (0.49% increase) were identified as part of DMN when ν increased from 0.31 to 0.41, indicating approximately 20 times less dependence on ν than OCSVM. The method was compared with the correlation analysis using the false discovery rate (FDR) control and independent component analysis (ICA) methods. The comparison was made under a comparable level of detection sensitivity in a predefined 10×6 voxels area in VACC, as shown in the encircled region in Fig. 3 (c). For comparison, the thresholds of correlation analysis and ICA were adjusted to detect the same number of voxels in this region. In the ICA analysis, all independent components (IC) were visually inspected and those corresponding to the DMN were combined to form the network map. Fig. 3 (e) and (f) show the network maps identified by the correlation analysis and ICA. It was observed in Fig. 3 (e) that connected voxels in the right inferior parietal cortex were under-detected by

the correlation analysis. Significant over-detections were also found around the medial prefrontal cortex identified by ICA, as shown in Fig. 3 (f).

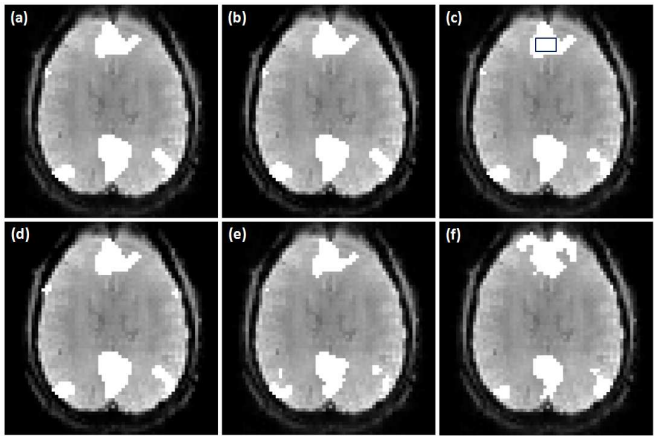

Fig. 3. Part of DMN detected from a subject in the resting state experiment using the proposed method with ν = (a) 0.31, (b) 0.37, (c) 0.39, (d) 0.41, and using (e) the correlation analysis with the FDR control and (f) ICA. The encircled rectangular region in (c) indicates a 10×6 voxels area in VACC. The thresholds of correlation and ICA methods were adjusted to detect all voxels in this region.

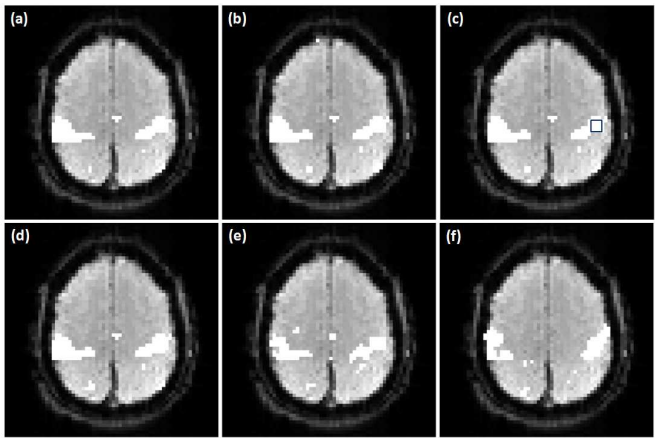

Fig. 4. Part of SMN detected from the same subject as shown in Fig. 3 using the proposed method with ν = (a) 0.25, (b) 0.29, (c) 0.31, (d) 0.35, and using (e) the correlation analysis with the FDR control and (f) ICA. The encircled region in (c) indicates a 4×4 voxels rectangular area in M1. The thresholds of correlation and ICA methods were adjusted to detect all voxels in this region.

Fig. 4 shows part of sensorimotor network (SMN) detected from the same data but a different slice as that shown in Fig. 3. Fig. 4 (a)-(d) are the network maps identified by the proposed method using ν =0.25, 0.29, 0.31, and 0.35, respectively. There are 1356 voxels in this slice involved to the analysis. Only 12 more voxels (0.88%) were detected as part of SMN when ν increased from 0.25 to 0.35, indicating about 11.36 times less dependence on ν than OCSVM. The encircled rectangular region in (c) is a 4×4 voxels area in the primary motor cortex (M1). The thresholds of correlation analysis and ICA were changed to identify the same number of voxels in this region. Fig. 4 (e) and (f) show the SMN maps detected using the correlation analysis and ICA. The results of the correlation analysis and proposed method are close to each other. An under-detection in the supplementary motor cortex was observed from the map generated by ICA. This under-detection is not because of a missing of SMN-related ICs, but is due to the thresholding of ICs to generate the same detection sensitivity in M1 as the proposed method.

V. Conclusions

A SVM-based method was developed for a unified analysis of task-related and resting state fMRI data. The innovation is to formulate the mapping of active/connected voxels as an outlier detection process, based on which the analysis of task-related or resting state data is performed using the same machine learning framework. The method does not reply on a threshold for the final decision, and can adapt to intra- and inter-subject variation of fMRI data. The experimental results indicate that the method can provide consistent mapping of active/connected voxels, and comparable or better results than the correlation and ICA methods. It is applicable to various quantitative fMRI studies. The future work will be focused on the method evaluation using more experimental data, and the extending of the method to the activation/functional connectivity detection at group level.

References

[1] C. Tegeler, S. Strother, R. Anderson, and S. Kim, "Reproducibility of BOLD-based functional MRI obtained at 4T," *Human Brain Mapping*, vol. 7, pp. 267–283, 1999.

[2] J. Voyvodic, J. Petrella, and A. Friedman, "fMRI activation mapping as a percentage of local excitation: consistent presurgical motor maps without threshold adjustment," *Journal of Magnetic Resonance Imaging*, vol. 29, pp. 751–759, 2009.

[3] X. Song and A. Wyrwicz, "Unsupervised spatiotemporal fMRI data analysis using support vector machines," *NeuroImage*, vol. 47, pp. 204–212, 2009.

[4] A. Laird, J. Lancaster, and P. Fox, "Brainmap: The social evolution of a human brain mapping database," *Neuroinformatics*, vol. 3, pp. 65–78, 2005.

[5] A. Laird, P. Fox, S. Eickhoff, and et al., "Behavioral interpretations of intrinsic connectivity networks," *Journal of Cognitive Neuroscience*, vol. 12, pp. 4022–4037, 2011.

[6] S. Smith, P. Fox, and et al., "Correspondence of the brain's functional architecture during activation and rest," *PNAS*, vol. 106, no. 31, p. 13040?13045, 2009.

[7] M. Jenkinson, P. Bannister, J. Brady, and S. Smith, "Improved optimisation for the robust and accurate linear registration and motion correction of brain images," *NeuroImage*, vol. 17, no. 2, pp. 825–841, 2002.

[8] X. Song, M. Murphy, and A. Wyrwicz, "Spatiotemporal denoising and clustering of fMRI data," in *Proc. IEEE Int. Conf. Image Process.*, 2006, pp. 2857–2860.

[9] K. Friston, A. Holmes, and et al., "Statistical parametric maps in functional imaging: a general linear approach," *Hum. Brain Mapp.*, vol. 2, p. 189?210, 1995.

[10] T. Evgeniou, M. Pontil, C. Papageorgiou, and T. Poggio, "Image representations and feature selection for multimedia database search," *IEEE Trans. on Knowledge and Data Engineering*, vol. 15, no. 4, pp. 911–920, 2003.

[11] V. N. Vapnik, *Statistical learning theory*. Wiley-Interscience, 1998.

[12] B. Schölkopf and A. Smola, *Learning with kernels: support vector machines, regularization, optimization, and beyond*. MIT Press, 2001.

[13] B. Schölkopf, J. Platt, J. Shawe-Taylor, A. Smola, and R. Williamson, "Estimating the support of highdimensional distribution," *Neural Computation*, vol. 13, no. 7, pp. 1443–1471, 2001.

[14] B. Dasarathy, J. Sanchez, and S. Townsend, "Nearest neighbour editing and condensing tools-synergy exploitation," *Pattern Analysis and Applications*, vol. 3, no. 1, pp. 19–30, 2000.

[15] T. Wu, C. Lin, and R. Weng, "Probability estimates for multi-class classification by pairwise coupling," *Journal of Machine Learning Research*, vol. 5, pp. 975–1005, 2004.